INSTITUTE OF PLASMA PHYSICS
CZECHOSLOVAK ACADEMY OF SCIENCES

COMMENTS ON EDGE TURBULENCE DURING LOWER HYBRID CURRENT DRIVE EXPERIMENT ON CASTOR TOKAMAK

Stöckel J., Kryška L., Žáček F.
Institute of Plasma Physics Czech. Acad. of Sciences
Nanobashvili S.
Institute of Physics, Georgian Acad. Sci.

RESEARCH REPORT

IPPCZ-279

March1988

POD VODÁRENSKOU VĚŽÍ 4, 180 69 PRAGUE 8
CZECHOSLOVAKIA

COMMENTS ON EDGE TURBULENCE DURING LOWER HYBRID CURRENT DRIVE EXPERIMENT ON CASTOR TOKAMAK

Stöckel J., Kryška L.. Žáček F.
Institute of Plasma Physics Czech. Acad. of Sciences

Nanobashvili S.
Institute of Physics, Georgian Acad. Sci.

IPPCZ-279

March 1988

I. Introduction

In present-day tokamaks, the experimentally determined electron confinement time is roughly two orders of magnitude lower than the neoclassical prediction. A recent review of turbulence and anomalous transport /1/ identified both magnetic and electrostatic turbulences as candidates for inducing anomalous transport, but also concluded that their relative importance is unknown up to now.

However, the latest experiments on TEXT tokamak /2/, /3/ suggest a rather close correlation between the edge particle transport and electrostatic turbulence in Ohmical heating (OH) regimes. The similar indications have been found on the other tokamaks as CALTECH /4/, TOSCA /5/, TV-1 /6/, PRETEX /7/, and MACROTOR /8/. On the other hand, some experimental evidence that the magnetic fluctuations may be connected to anomalous energy losses has been given in other tokamaks as well. Especially in additionally heated plasmas on JET /9/ and ASDEX /10/ a posible link between the energy confinement and magnetic fluctuation level has been observed. Generally, the magnetic fluctuations' level reveals a systematic increase of magnetic activity with decreasing τ_e^E, if an additional heating (namely neutral beam injection and ion cyclotron resonance heating) is applied. In the similar way, an additional heating on TFR leads to the simultaneous increase of the density fluctuations' level in the central part of the plasma column and the thermal conductivity of the electron component.

The study of energy and particle confinement during lower hybrid current drive (LHCD) regimes has only recently begun and there is relatively a little information available at the present. However, there are some indications, namely in regimes with a combined inductive and LH current drive (LHCD/OH) that the particle confinement (T-7 /12/; VERSATOR II /13/, /14/) and energy confinement (T-7 /15/, ALCATOR /16/, PLT /17/, PETULA B /18/, ASDEX /19/) are improving under some experimental conditions, namely when the additional RF power at moderate power levels ($P_{RF} \lesssim P_{OH}$) is applied.

Nevertheless, any correlations between the improvement of the particle/energy confinement and the electrostatic/magnetic turbulence have not yet been investigated experimentally in the case of LHCD/OH regimes.

Some indications of improvement of the particle confinement have been observed during the combined LHCD/OH regimes on the CASTOR tokamak as well /2/. Here we report the preliminary results concerning with a possible link between the improvement of the particle confinement and decrease of the level of electrostatic turbulence at the periphery of the plasma column, which are routinely observed on the CASTOR tokamak during the combined LHCD/OH regimes.

The report is organized as follows: Description of experiment including the discussion of Langmuir probe diagnostics is presented in Section II. The preliminary experimental results concerning with some characteristic features of the edge electrostatic turbulence in OH regime are compared with that of LHCD/OH

plasmas in Section III. The results are discussed in connection with an improvement of particle confinement in Section IV and summarized in Section V.

II. Experimental arrangement

Discharge conditions: The experiment was performed on the CASTOR tokamak /21/, a small device (R = 0.4 m, a = 0.085 m, B = 1.3 T) with the iron core transformer and copper shell, at plasma current I_p = 12 kA. The duration of the discharge is about 9 ms. One poloidal aperture limiter (Mo) and two movable rail limiters (one from the top, the second from the bottom) are located at the same toroidal position as a gas fuelling of the discharge. The stable low density discharge ($\bar{n}_e \lesssim 10^{19}$ m^{-3}), necessary for the efficient LHCD, can be successively established only without any impulse gas puffing. In this case the line-average density decreases during the discharge roughly exponentially with a time constant $\sim$ 3 ms. Due to the imperfect stabilization, the position of the plasma column is changing in time, namely during the anomalous Doppler instability, which is routinely present in our low density plasmas /22/.

LHCD system: The two antenna systems (multijunction waveguide grills /23/) have been used for radial launching of the lower hybrid waves (f = 1.25 GHz) into the plasma (see fig. 1). The first multijunction grill G_4 consists of four waveguides, phase shifted by 120 °, and according the computation its spectrum peaks at $N_{\parallel} \doteq 5$. The second grill G_7, with seven adjacent wave-

guides, has maximum at $N_{\parallel} \doteq 10$. Each grill is feeded by one magnetron with a net power of about $P_{RF} = 40$ kW.

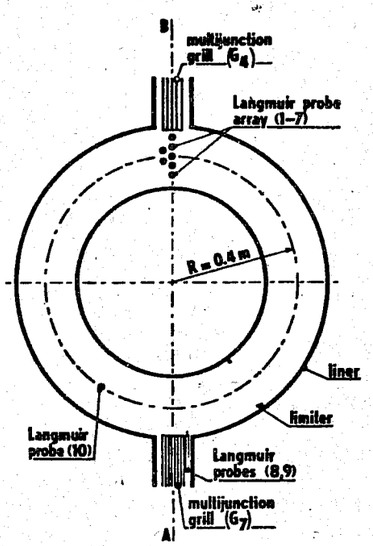

Fig. 1. The top view of the CASTOR tokamak with two multijunction waveguide grills G_4 and G_7.

Diagnostics: The experiment is equipped by a standard set of diagnostics. As usual, the current drive efficiency is deduced from a drop of the loop voltage. The line average density is measured by a 4-mm interferometer over the central chord. The spectral line intensities are monitored by a visible monochromator at the limiter section, by a VUV monochromator (100 ° toroidally away from the electron side of the limiter) and by a photomultiplier with an interference filter (H_α -line viewing the mouth of the grill G_7.

Positions of Langmuir probes used for monitoring of edge fluctuations are depicted in fig. 2.

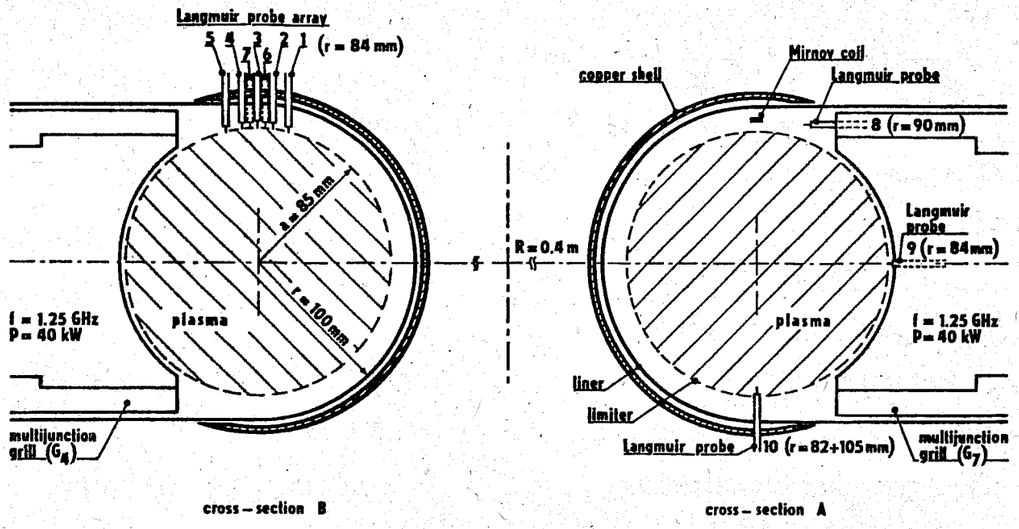

Fig. 2. Cross-sections of the liner through the grills G_4 and G_7.

A fixed probe array is located at r = a = 85 mm in the region of G_4-grill. It consists of five probes P_1 - P_5 separated poloidally by the distance $\Delta x = 4.5$ mm and probes P_6 and P_7 with the same separation but displaced 4 mm toroidally away from P_1 - P_5. Each probe is a 1 mm diameter molybdenum wire which extends 4.5 mm beyond a stainless steel shield 2.5 mm in diameter. A recessed glass covering provides insulation between the wire and the shield. The two fixed probes P_8, P_9 are mounted on G_7-grill at radii $r_8 = 90$ mm and $r_9 = 84$ mm. The radial profiles can be reconstructed by moving the probe P_{10} radially shot by shot.

The electron density n_e is derived from the probe ion saturation current I^+

$$n = I^+ \cdot \frac{2}{e.A} \cdot \sqrt{\frac{m_i}{k T_e}}\,, \qquad (1)$$

where A is probe surface area, m_i is the ion mass, $k = 1.6\text{x}10^{-19}$J/eV, $e = 1.6022\text{x}10^{-19}$C.

The space potential φ_s of the plasma follows from the floating potencial of the probe φ_f /2/

$$\varphi_s = \varphi_f + \frac{kT_e}{2|e|} \cdot \ln\left(\frac{m_i}{m_e}\right). \qquad (2)$$

Each measurement requires the electron temperature T_e for interpretation. However, the T_e was not measured in this series of experiments. For preliminary interpretation we have adopted our previous experimental data /24/ indicating the electron temperature in the range of 20 - 25 eV in the scrape-of-layer (SOL). This value seems to be independent (within the experimental errors) on radius in this region.

A probe, biased minus 150 V with respect to the liner, measures the ion saturated current. An unbiased probe is used to measure the plasma floating potencial. The voltage of each floating probe with respect to the liner is measured on the resistor 10 kΩ of a divider 1 : 100.

The important quantities from the point of view of electrostatic turbulence are the root-mean-square values of density and space potencial fluctuations defined as

$$\tilde{n} = \sqrt{\lim_{T\to\infty} \frac{1}{T}\int_0^T (n^f)^2 dt} \quad ; \quad \tilde{\varphi}_s = \sqrt{\lim_{T\to\infty} \frac{1}{T}\int_0^T (\varphi_s^f)^2 dt}, \qquad (3)$$

where subscript "^{f}" denotes fluctuating part and brackets $\langle\cdots\rangle$ further mean the time-average value of the corresponding quantity. The rms values of n and φ_s are deduced from the probe measurements of $\tilde{I}_s$ and $\tilde{\varphi}_f$ using the expressions (1) and (2), where

the electron temperature fluctuations $\tilde{T}_e$ are neglected according to the experimental evidence given in /25/ ($\tilde{T}_e/\langle T_e\rangle \lesssim 15$ %) or /5/ ($\tilde{T}_e/\langle T_e\rangle \lesssim 1$ %).

III. Experimental results

The typical temporal evolution of the ion saturated current during the combined LHCD/OH discharge is depicted in fig. 3 (upper trace of the oscillogram).

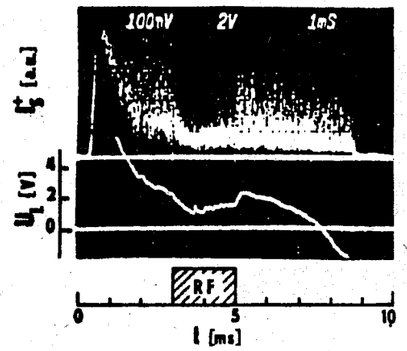

Fig. 3. The temporal evolution of the ion saturated current and loop voltage during the combined LHCD/OH discharge. The RF-pulse is applied at t = 3 - 5 ms. The probe P_8 and grill G_7 are used.

The drop of the loop voltage (lower trace of the oscillogram), just in the time of the RF-pulse, indicates that about one half of the toroidal current is driven by lower hybrid wave.

The relative level of fluctuations of the ion saturated current $\tilde{I}^+/\langle I^+\rangle$ (e.g. local electron density) inside of the SOL reaches a rather high value 0.5 - 0.8 during the OH-part of the discharge. That may be seen from fig. 4, where the radial profile

of the relative level of the density fluctuations $\tilde{n}/\langle n \rangle$ is depicted together with the radial profile of the time-average density $\langle n \rangle$. Note, that the absolute values of gradient scale length $L_n = \left(\frac{dn}{dr} \cdot \frac{1}{n}\right)^{-1}$ and $\tilde{n}/\langle n \rangle$ are not influenced by the choise of $T_e(r)$.

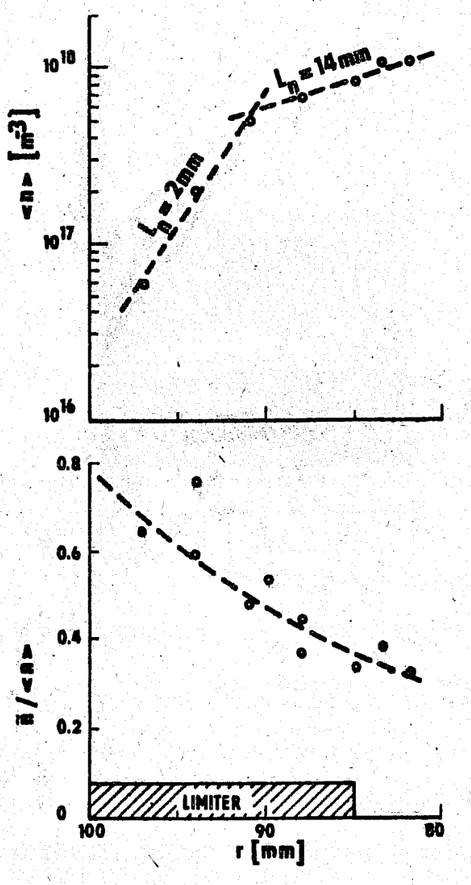

Fig. 4. The radial profiles of $\langle n \rangle$ and $\tilde{n}/\langle n \rangle$ in OH-discharge; probe P_{10}.

Let us add that the rms value of the floating potential measured in OH-discharges has been found in a range of 7 ÷ 10 V

at the plasma edge (r = a) and it increases towards the plasma core.

An attempt to obtain the frequency spectrum of the density fluctuations by a numerical Fourier analysis is shown in fig. 5, together with the spectrum of the potential fluctuations from the floating probe.

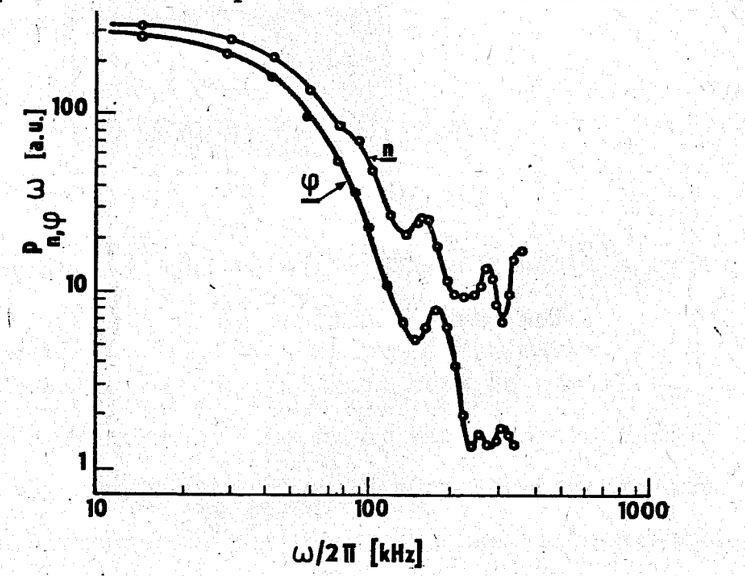

Fig. 5. The frequency spectra of the n- and φ_f - fluctuations at r = a, taken during the OH-part of the discharge; probe P_9.

In spite of incomplete experimental data, the figs. 4 and 5 indicate that the electrostatic edge turbulence on the CASTOR tokamak has in OH-regimes a similar character as on the other tokamaks /1/. That follows from the absolute value of the density fluctuations, from the noticeable decrease of their relative level towards the centrum of the plasma column and from the general form of the frequency spectra of n- and φ_f - fluctuations as well.

During the combined LHCD/OH period of the discharge the level of density fluctuations decreases remarkably. The detail

picture of the ion saturated current, taken just in the middle of the RF-pulse, is shown in fig. 6, where the comparison between the pure OH and combined LHCD/OH current drives is presented.

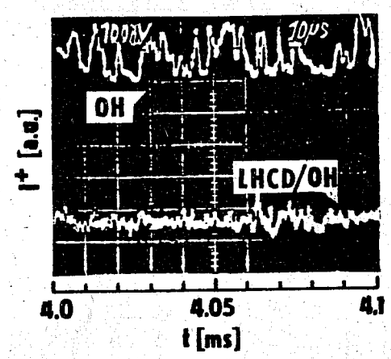

Fig. 6. The detail picture of the I^+-fluctuations, taken under the same conditions as in fig. 3.

It may be seen from fig. 6 that predominantly low frequency oscillations in the range 10 - 50 kHz are suppressed by RF. On the other hand, some high frequency (but low level) oscillations appear. The last statement can be supported by measurement of the frequency spectra of the I^+-fluctuations by a spectrum analyzer. Comparison of the spectra in the pure OH and combined LHCD/OH discharges is shown in fig. 7.

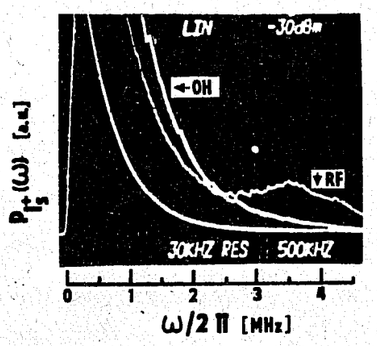

Fig. 7. The frequency spectra of I^+-fluctuations from the spectrum analyzer, type Tektronix 7L12.

It is possible to see that suppression of the low frequency part of the spectrum in the case of LHCD/OH regime is accompained by formation of a rather broad peak at frequencies in the range of 2 - 4 MHz. But it should be noted that the type of analyzer used is not very suitable for the sub-MHz region and so the presented result should be taken qualitatively only.

It has been investigated further, whether the effect of suppression of density fluctuations is dependent on the Langmuir probe position with respect to the waveguide grill. But using various probes in combination with grills G_4 and G_7 we have always obtained very similar results. Therefore, it has been concluded that the stabilizing effect is roughly toroidally symmetric. However, there were some indications that the suppression of fluctuations is more pronounced at the top of the torus e.g. in direction of the toroidal drift of ions. This fact suggests some poloidal asymmetry. But this question should be study in more detail in future.

Further, there were monitored the differential signals from two floating probes of the probe array. The probes are located on the same radius with respect to the center of the liner. Therefore, as follows from eq. (2), the differential signal corresponds to the difference of the space potentials $\varphi_s^x - \varphi_s^y$, since the terms containing the electron temperature cancel out. An estimate of the value of the poloidal electric field E_p can be simply obtained by dividing $\Delta\varphi_s = \varphi_f^x - \varphi_f^y$ by the distance of the probes Δx. Fig. 8 demonstrates the dependence of the differential signal of two probes on their distance and the influence of the RF-power

on the fluctuation level. The rms value of the E_p-fluctuations, estimated from the adjacent probes $\Delta x = 4.5$ mm is in the range of 1 - 1.5x10^3 V/m in OH regime. Comparison of ΔI_s-signals for different probe pairs in the OH and LHCD/OH regimes clearly manifests a substantial decrease of the fluctuation level under LHCD for all distances which were used. However, the stabilizing effect is most pronounced for the adjacent probes.

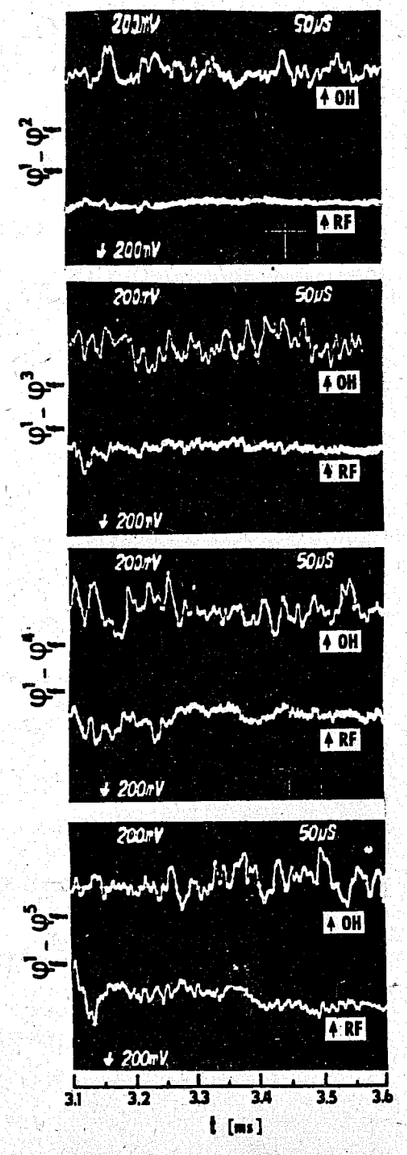

Fig. 8. The differential signal of the two floating probes for Δx = 4.5, 9, 13.5 and 18 mm (down from the top) in OH and LHCD/OH regimes. The RF-power from grill G_7 is applied at t = 2.9 ms. The measurement has been performed within the limited frequency bandwidth $\omega/2\pi < 100$ kHz.

The analogical decrease of the poloidal magnetic field fluctuations during LHCD/OH discharge has been observed on the signals from Mirnov coils located inside the SOL (see fig. 9). In this figure the signal from a floating probe is given for comparison as well. Analogical suppression of the MHD-activity (identified as stabilization of m = 2 mode) in LHCD/OH regimes has been previously reported on the PETULA B tokamak /26/.

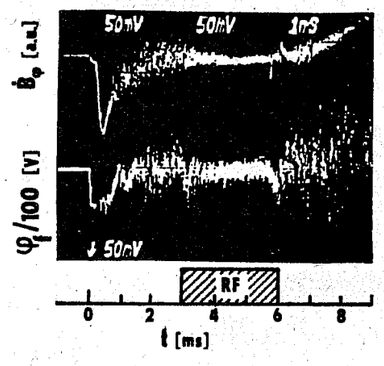

Fig. 9. Derivative of the poloidal magnetic field B and floating potential φ_f during the combined LHCD/OH discharge.

IV. Discussion

In the combined LHCD/OH regimes the global particle confinement time increases in our case approximately two times with respect to the pure OH- ischarge /20/. This effect, observed earlier under similar experimental conditions on VERSATOR /13/ and T-7 /12/ tokamaks, is demonstrated by the temporal evolution of the line-average electron density, see fig. 10.

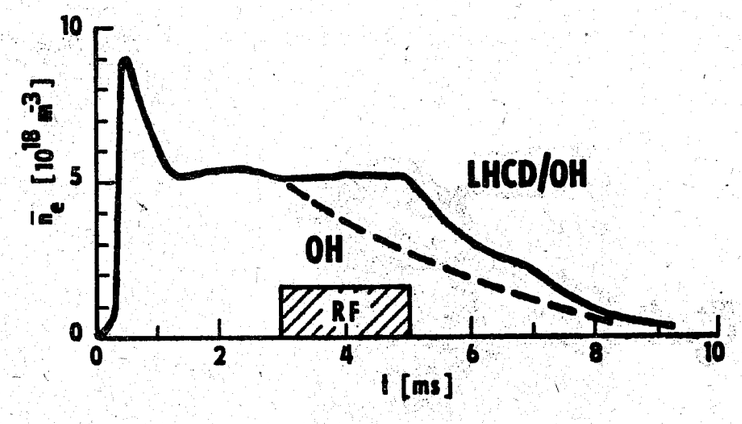

Fig. 10. The temporal evolution of the line-average density during combined LHCD/OH regime. The same curve for pure OH-discharge is shown by dashed line for comparison.

The density reaches its maximum at t = 1 ms, when the plasma is fully ionized. After that density decreases due to the finite particle confinement and due to the fact that the recycling coefficient is well bellow one. The rate of decrease depends predominantly on the degree of wall conditioning. For the low density discharges without impulse gas puffing, which are favourable for LH-current drive, the global particle confinement time has been found in the range of 2 ms from the both density and absolute intensity of a hydrogen spectral line measurements. During the LHCD/OH part of the discharge the continuous decrease of the density is stopped. The density starts to be constant or even slightly increases. The spectroscopic measurements indicate that neither an additional ionization of hydrogen fluxes (from wall, limiter or grill) nor the additional ionization of impurities are responsible for this relative increase of the density. The last is therefore interpreted as an improvement of the global particle confinement.

Taking into account simultaneous existence of the density stabilization and the edge plasma turbulence suppession during the combined LHCD/OH discharge, it seems to be natural to link both these effects together. Such attempt is presented in the following subsection.

<u>The fluctuation — induced particle transport</u>

The experimentally observed fluctuations of the poloidal electric field E_p^f lead to fluctuations of the particle velocities and radial positions /1/. For low-frequency fluctuations ($\omega \ll \omega_{ci}$) a radial velocity fluctuation v_r^f of particle can be written

$$\vec{v}_r^{\,f} = \frac{\vec{E}_p^{\,f} \times \vec{B}}{B^2}\,, \qquad (4)$$

where $\vec{B}$ is toroidal magnetic field.

To express a time average radial particle flux $\langle \Gamma \rangle = \frac{\langle n \cdot \vec{v}_r \rangle}{B}$ given by the cross-field drift, it is necessary to know a correlation between the radial velocity fluctuations and plasma density fluctuations n^f as

$$\langle \Gamma \rangle = \frac{1}{B}\left\langle (\langle n \rangle + n^f)(\langle E_p \rangle + E_p^f) \right\rangle = \frac{1}{B}\langle n \rangle \langle E_p \rangle + \frac{1}{B}\langle n^f \cdot E_p^f \rangle .$$

As there is no experimental evidence about existence of the quasistacionary poloidal electric field $\langle E_p \rangle$, the first term of the last expression may be neglected. It means, the cross-field contribution to the radial transport has only a turbulent part, which can be writen as

$$\Gamma^t = \frac{1}{B} \lim_{T\to\infty} \frac{1}{T} \int_0^T n^f \cdot E_p^f \, dt\,, \qquad (5)$$

or using a cross-correlation coefficient C_{nE} /4/ as

$$\Gamma^t = \frac{1}{B} \cdot C_{nE} \cdot \tilde{n} \cdot \tilde{E}_p\,. \qquad (6)$$

The definition of C_{nE} follows directly from expressions (5), (6) and its value is between -1 and +1. The polarity of C_{nE} determins the direction of the net turbulent flux. Many tokamak experiments /2 - 8/ have shown that the net turbulent flux at the plasma edge has always outwards direction. The absolute value of C_{nE} has been found in the range of 0.2 - 0.4, which indicates nearly complete de-correlation between density and E_p-fluctuations.

Now, assuming quasineutrality, we can express the fluctuation-induced diffusion coefficient D^t as

$$D^t = -\Gamma^t / \nabla n = - C_{nE} \cdot \frac{\tilde{n}}{\langle n \rangle} \cdot \frac{\tilde{E}_p}{B} \cdot L_n\,, \qquad (7)$$

Here $\tilde{n}/\langle n \rangle$ is the relative level of density fluctuations and $L_n = n/\nabla n$ is the density gradient scale length. If we take the typical experimental values for plasma edge of the CASTOR tokamak: $E_p = 1.5 \times 10^3$ V/m, $B = 1.3$ T, $n/\nabla n = 0.4$, $L_n = 1.4 \times 10^{-2}$ m and supposing $C_{nE} = 0.3$, we get for coefficient of turbulent diffusion at the limiter radius the value $D^t = 2$ m^2/s, which is in the range of Bohm diffusion $D_{Bohm} = 0.0625\, T_e/B = 1$ m^2/s.

Moreover, assuming further the poloidal and toroidal symmetry of the turbulent particle flux Γ^t through the outermost closed magnetic surface, the fluctuation-induced global particle confinement time τ_p^t can be estimated according to its definition $\tau_p^t \cdot \int_S \Gamma^t dS = \int_V n \, dV$ as following:

$$\tau_p^t = \frac{a}{2} \cdot \frac{n_v}{\Gamma^t(a)} = \frac{3}{8} \cdot \frac{a \cdot B}{C_{nE} \cdot \tilde{E}_p} \cdot \frac{\bar{n}/\langle n(a) \rangle}{\tilde{n}/\langle n(a) \rangle}\,.$$

Here volume averaged density n_v is related to the measured line average value $\bar{n}$ as $n_v = (3/4)\bar{n}$ assuming parabolic profile of $n(r)$.

We have found the ratio line-average/peripheral density $\bar{n}/\, n(a)$ to be in the range of $5 \div 10$ for $r = a = 85$ mm. Therefore, the estimated fluctuation-induced global particle confinement time is in the range of 1.1 - 2.3 ms. It well corresponds to the spectroscopic data.

It may be concluded from the given above that the fluctuation-induced transport seems to be responsible for the anomalous particle losses on the CASTOR tokamak. Analogical conclusion has been done on some other tokamak experiments as well /2 - 8/. The simultaneous decrease of the relative level of density and poloidal field fluctuations during the combined LHCD/OH regimes may therefore result in a noticeable improvement of the particle confinement (assuming of course that the cross-correlation coefficient C_{nE} doesn't increase appreciably). This idea is supported by the global particle balance measurements which manifest an increase of the global particle confinement time as well.

However, it should be noted that more quantitative conclusions need determination of the cross-correlation coefficient or at least the simultaneous measurement of rms values of the poloidal field and density fluctuations. Moreover, for comparison of turbulent losses with global particle balance the dependence of the turbulent flux on the poloidal angle has to be measured. Such experiments are under preparation in the CASTOR tokamak.

V. Summary:

(i) The preliminary measurements of the plasma edge fluctuations on the CASTOR tokamak are presented.

(ii) The level of the edge turbulence has been found sufficiently high to explain anomalous particle losses in the OH-discharge in tokamak.

(iii) The level of the edge turbulence decreases appreciably during the combined LHCD/OH regimes. This fact indicates an improvement of the particle confinement which is observed by the other diagnostic tools as well.

ACKNOWLEDGEMENTS

The authors wish to thank J. Michálek and M. Vošvrda for calculation of fluctuation spectra in Fig. 5.

References

/1/ Liewer P. C.: Nucl. Fus. 23, 1983, No. 5, p. 543 - 621.

/2/ Rowan W. L. et al.: Nucl. Fus. 27, 1987, No. 7, p. 1105 - 1118.

/3/ Ritz C. P. et al.: Nucl. Fus. 27, 1987, No. 7, p. 1125 - 1134.

/4/ Zweben S. J., Gold R. W.: Nucl. Fus. 25, 1985, No. 2., p. 171 - 183.

/5/ Howlings A., Coté A., Doyle E. J., Evans D. C., Robinson D.C.: In Proc. XIIth European Conference on Controlled Fusion and Plasma Physics, Vol. 1, p. 311 - 314, Budapest, 1985.

/6/ Budaev V. P., Ivanov R. S.: In Proc. XIIth European Conference on Controlled Fusion and Plasma Physics, Vol. 1, p. 303 - 306, Budapest, 1985.

/7/ Levinson S. J., Beall J. M., Powers E. J., Bengston R. D.: Nucl Fus. 24, 1984, No. 5, p. 527 - 539.

/8/ Zweben S. J., Taylor R. J.: Nucl. Fus. 23, 1983, No. 4, p. 513 - 528.

/9/ Malacarne M., Duperrex P. A.: Report JET-P(87)26, May 1987

/10/ Dodel G., Holzhauer E., Massig J., Gernhardt J. and ASDEX-, ICRH-, LH-, NI- and Pellet-Teams: Report IPP III/120, June 1987, Garching, p. 59 - 63.

/11/ Olivain J. et al.: Report EUR-CEA-FC-1325, April 1987.

/12/ Alikaev V. V., Gvozdkov J. V., Ďatlov J., Žáček F., Ivanov D. P., Ilin V. I., Kakurin A. M., Kopecký V., Kočin V. A., Kislov A. J., Klíma R., Kovrov P. E., Neudachin C. V., Preinhaelter J., Chvostenko P. P., Chromkov I. N., Chistjakov V. V., Stöckel J., Jakubka K.: Fizika plazmy 11, 1985, No 1., p. 53 - 61.

/13/ Luckhardt S. C. et al.: Phys. Fluids 29/6/, 1986, No 6, p. 1985 - 1993.

/14/ Mayberry M. J., K.I. Chen, Luckhardt S. C., Porkolab M.: Phys. Fluids 30, 1987, No 7., p. 2288 - 2291.

/15/ Alikaev V. V., Borschegovski A. A., Chistjakov V. V., Gorelov J. A., Ilin V. I., Ivanov D. P., Ivanov N. V., Kakurin A. M., Khvostenko P. P., Kislov A. J., Kochin V. A. Kovrov P. E., Likin K. I., Maksimov J. S., Semenev I. R., Shigaev A. P., Sokolov J. A., Vasin N. L., Volkov V. V., Ďatlov J., Kopecký V., Kryška L.: In Proc. of XIth International Conference on Plasma Physics and Controlled Nuclear Fusion Research, Kyoto, Japan, 13 - 20 November 1986, Paper IAEA-CN-47/F-II-4.

/16/ Takase Y. et al.: Nucl. Fus. 27, 1987, No 1., p. 53 - 64.

/17/ Stevens J. E. et al.: Proc. 12th Eur. Conf. on Contr. Fus. and Plasma Phys., Budapest 1985, Vol. II, p. 192.

/18/ Parlange F. et al.: Proc. 12th Eur. Conf. on Contr. Fus. and Plasma Phys., Budapest 1985, Vol. II, p. 172.

/19/ Söldner F. et al.: Proc. 12th Eur. Conf. on Contr. Fus. and Plasma Phys., Budapest 1985, Vol. II., p. 244.

/20/ Badalec J.: In Proc. of 13th Czechoslovak seminar on plasma physics and technology, Liblice, Czechoslovakia, March 1987.

/21/ Djabilin K. S., Badalec J., Borschegovski A. A., Ďatlov J., Jakubka K., Kopecký V., Korotkov A. A., Stöckel J., Valovič M., Žáček F.: Czech. J. Phys. B 37, 1987, p. 713.

/22/ Valovič M.: Czech. J. Phys. B 38 (1988) 65.

/23/ Žáček F., Badalec J., Ďatlov J., Jakubka K., Kopecký V., Kryška L., Magula P., Preinhaelter J., Stöckel J., Valovič M.: IAEA Technical Committee Meeting on Research Using Small Tokamaks, Nagoya, 10 -12 Nov. 1986.

/24/ Jakubka K., Stöckel J., Žáček F., Nanobashvili S.: Czech. J. Phys. B 33, 1983, p. 663.

/25/ Liewer P. C., McChesney J. M., Zweben S. J., Gould R. W.: Phys. Fluids 29/1/, 1986, p. 309.

/26/ Van Houtte D. et al.: Nucl. Fus. 24, 1984, No 11., p. 1485 - 1489.